Control of Structural Isomerism in Noncovalent Hydrogen-Bonded Assemblies Using Peripheral Chiral Information

Leonard J. Prins, Katrina A. Jolliffe, Ron Hulst, Peter Timmerman,* and David N. Reinhoudt*

Contribution from the Laboratory of Supramolecular Chemistry and Technology, MESA+ Research Institute, University of Twente, P.O. Box 217, 7500 AE, Enschede, The Netherlands

Received October 8, 1999

Abstract: The results of a systematic study of the structural isomerism in more than 30 noncovalent hydrogen-bonded assemblies are described. These dynamic assemblies, composed of three calix[4]arene dimelamines and six barbiturates/cyanurates, can be present in three isomeric forms with either D_3, C_{3h}, or C_s symmetry. The isomeric distribution can be readily determined via a combination of ^{1}H NMR and ^{13}C NMR spectroscopy. In one case it is shown that the covalent capture of the dynamic assemblies via a ring-closing metathesis (RCM) reaction provides a novel analytical tool to distinguish between the D_3 and C_{3h} isomeric forms of the assembly. For the D_3 isomer the RCM results in the formation of a cyclic trimer, comprising three dimelamines, whereas for the C_{3h} isomer a cyclic monomer is formed. Molecular dynamics simulations in chloroform are qualitatively in agreement with the experimental data and reveal that the isomeric distribution is determined by a combination of steric, electronic, and solvation effects. A wide range of isomeric distributions covering all extremes has been found for the studied assemblies. Those with 5,5-disubstituted barbituric acid derivatives exclusively form the D_3 isomer, because steric hindrance between the barbiturate substituents prevents formation of the C_{3h} and C_s isomers. In contrast, assemblies with isocyanuric acid derivatives exhibit increased stability of the C_{3h} and C_s isomers upon increasing the size of the isocyanurate substituent. The outcome of the assembly process can be controlled to a large extent via chiral substituents in the calix[4]arene dimelamines, due to the preferred orientation of the chiral centers.

Introduction

Noncovalent interactions play an important role in determining the three-dimensional structure of biological assemblies.[1] Although only a limited number of building blocks are used, the structural variety in these assemblies is enormous. Examples are the various forms of DNA[2] and the α-helices or β-sheets in proteins.[3] Subtle changes in the arrangement of the building blocks can have a large effect on the secondary structure of proteins, as was recently demonstrated by Sauer et al.[4] The interchange of just two amino acids in the Arc repressor completely changes the secondary structure of the protein from a β-sheet to a right-handed helix. Similar forms of structural isomerism have been observed in synthetic noncovalent assemblies, which are the subject of numerous studies[5] because they offer new perspectives in the fields of catalysis,[6] guest encapsulation,[7] and combinatorial chemistry.[8] Whitesides recognized that there are three different structural motifs in the isocyanuric acid·melamine (CA·M) lattice, i.e., the linear and crinkled tape motif and the cyclic rosette motif.[9,10] Structural isomerism has also been observed within other well-defined molecular assemblies as a result of different orientations of the building blocks within the assembly[11] or as a result of tautomerism.[12] These forms of structural isomerism often result in the formation of a mixture of assemblies. This always complicates the analysis and will eventually affect the application of this type of self-assembled structures.

* To whom correspondence should be addressed.

(1) Stryer, L. *Biochemistry*; W. H. Freeman: New York, 1995.

(2) Dickerson, R. E.; Drew, H. R.; Conner, B. N.; Wing, R. M.; Fratini, A. V.; Kopka, M. L. *Science* **1982**, *216*, 475−485

(3) Fersht, A. R. *Enzyme Structure and Mechanism*; W. H. Freeman: New York, 1985.

(4) Cordes, M. H. J.; Walsh, N. P.; McKnight, C. J.; Sauer, R. T. *Science* **1999**, *284*, 325−328.

(5) For reviews, see: (a) Conn, M. M.; Rebek, J., Jr. *Chem. Rev.* **1997**, *97*, 1647−1668. (b) Linton, B.; Hamilton, A. D. *Chem. Rev.* **1997**, *97*, 1669−1680. (c) Philp, D.; Stoddart, J. F. *Angew. Chem., Int. Ed. Engl.* **1996**, *35*, 1154−1196. (d) Lawrence, D. S.; Jiang, T.; Levett, M. *Chem. Rev.* **1995**, *95*, 2229−2260.

(6) For a short review, see: (a) Sanders, J. K. M. *Chem. Eur. J.* **1998**, *4*, 1378−1383. (b) Kang, J.; Santamaría, J.; Hilmersson, G.; Rebek, J., Jr. *J. Am. Chem. Soc.* **1998**, *120*, 7389−7390.

(7) (a) Kusukawa, T.; Fujita, M. *Angew. Chem., Int. Ed.* **1998**, *37*, 3142−3144. (b) MacGillivray, L. R.; Atwood, J. L. *Nature* **1997**, *389*, 469−472. (c) Rivera, J. M.; Martín, T.; Rebek, J., Jr. *Science* **1998**, *279*, 1021−1023. (d) Meissner, R. S.; Rebek, J., Jr.; De Mendoza, J. *Science* **1995**, *270*, 1485−1488. (e) Wyler, R.; De Mendoza, J.; Rebek, J., Jr. *J. Am. Chem. Soc.* **1993**, *32*, 1699−1701.

(8) For a short review, see: Timmerman, P.; Reinhoudt, D. N. *Adv. Mater.* **1999**, *11*, 71−74.

(9) Zerkowski, J. A.; Seto, C. T.; Whitesides, G. M. *J. Am. Chem. Soc.* **1992**, *114*, 5473−5475.

(10) (a) Mascal, M.; Hext, N. M.; Warmuth, R.; Moore, M. H.; Turkenburg, J. P. *Angew. Chem., Int. Ed. Engl.* **1996**, *35*, 2204−2206. (b) Lehn, J.-M.; Mascal, M.; DeCian, A.; Fischer, J. *J. Chem. Soc., Chem. Commun.* **1990**, 479−480. (c) Seto, C. T.; Whitesides, G. M. *J. Am. Chem. Soc.* **1990**, *112*, 6409−6411.

(11) (a) Hasenknopf, B.; Lehn, J.-M.; Boumediene, N.; Leize, E.; Van Dorsselaer, A. *Angew. Chem., Int. Ed.* **1998**, *37*, 3265−3268. (b) Castellano, R. K.; Kim, B. H.; Rebek, J., Jr. *J. Am. Chem. Soc.* **1997**, *119*, 12671−12672. (c) Fujita, M.; Ibukuro, F.; Yamaguchi, K.; Ogura, K. *J. Am. Chem. Soc.* **1995**, *117*, 4175−4176. (d) Mathias, J. P.; Simanek, E. E.; Whitesides, G. M. *J. Am. Chem. Soc.* **1994**, *116*, 4326−4340.

(12) (a) González, J. J.; Prados, P.; De Mendoza, J. *Angew. Chem., Int. Ed.* **1999**, *38*, 525−528. (b) Corbin, P. S.; Zimmerman, S. C. *J. Am. Chem. Soc.* **1998**, *120*, 9710−9711. (c) Beijer, F. H.; Sijbesma, R.; Kooijman, H.; Spek, A. L.; Meijer, E. W. *J. Am. Chem. Soc.* **1998**, *120*, 6761−6769.

10.1021/ja9936262 CCC: $19.00
Published on Web 04/05/2000

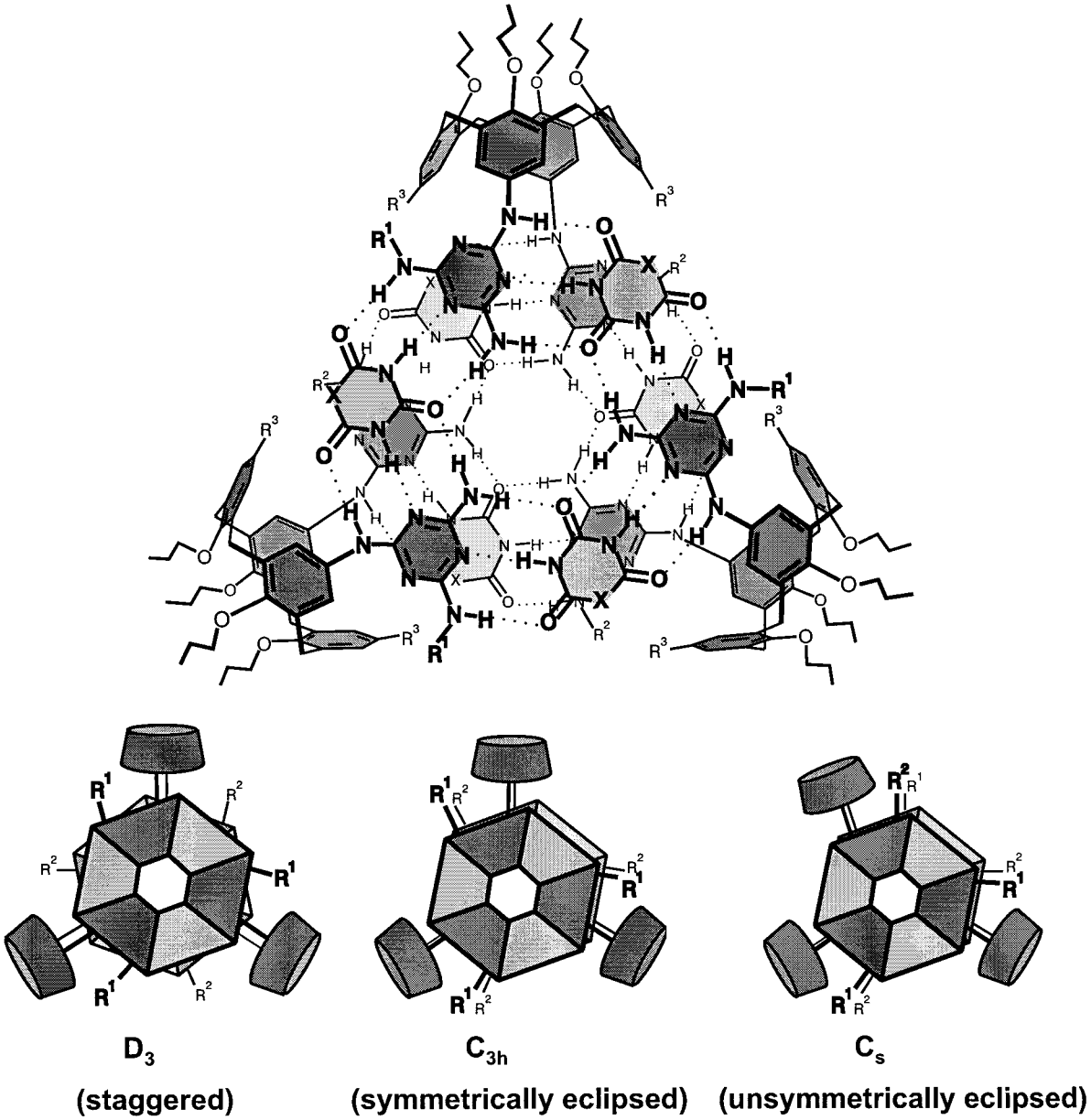

Figure 1. Molecular structure of double rosette assemblies such as $\mathbf{1}_3$·$(DEB)_6$ and the three structural isomers of this type of assembly.

In this paper we describe the results of a systematic study aimed at characterizing the various parameters that govern the isomeric distribution in a series of nine-component hydrogen-bonded assemblies. Understanding these parameters is essential in order to control the assembly process and to generate one (or more) of the isomers selectively. Initially, we will analyze the isomeric distribution in more than 30 different assemblies by ^{1}H and ^{13}C NMR spectroscopy and show that molecular dynamics simulations provide a qualitative insight into how the different parameters influence the isomeric distribution. Second, we show that the products formed after covalent capture of a dynamic assembly can be used to determine the symmetry of the assemblies, which renders it a useful analytical tool. Finally, we show how in certain cases the isomeric distribution of the assembly can be controlled via the introduction of chiral centers in the individual building blocks.

Results and Discussion

^{1}H and ^{13}C NMR Spectroscopic Characterization of the Isomers. Nine-component assemblies (e.g., $\mathbf{1}_3$·$(DEB)_6$) comprising three molecules of calix[4]arene dimelamine **1** and six molecules of 5,5-diethylbarbituric acid (DEB) are currently investigated in our group.[13] The driving force for the assembly process is the cooperative formation of 36 hydrogen bonds. In principle, assemblies such as $\mathbf{1}_3$·$(DEB)_6$ can be present as three constitutionally different isomers: the D_3 isomer (staggered), the C_{3h} isomer (symmetrically eclipsed), and the C_s isomer (unsymmetrically eclipsed) (Figure 1).

In the D_3 isomer the two melamine units of all three calix[4]arenes are in a staggered orientation with respect to each other (Figure 2), which causes the assembly to be chiral.[14]

(13) (a) Jolliffe, K. A.; Crego Calama, M.; Fokkens, R.; Nibbering, M. M.; Timmerman, P.; Reinhoudt, D. N. *Angew. Chem., Int. Ed. Engl.* **1998**, *37*, 1247−1251. (b) Timmerman, P.; Vreekamp, R. H.; Hulst, R.; Verboom, W.; Reinhoudt, D. N.; Rissanen, K.; Udachin, K. A. *Chem. Eur. J.* **1997**, *3*, 1823−1832. (c) Vreekamp, R. H.; Van Duynhoven, J. P. M.; Hubert, M.; Verboom, W.; Reinhoudt, D. N. *Angew. Chem., Int. Ed. Engl.* **1996**, *35*, 1215−1218.

(14) The orientation of the two melamines can either be clockwise (*P*) or counterclockwise (*M*). In the absence of additional chiral centers present in the building blocks, the staggered isomer exists as a racemic mixture of the *P* and *M* assembly.

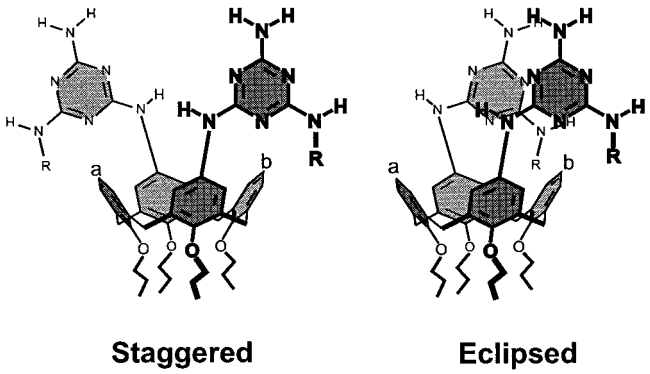

Figure 2. Staggered and eclipsed orientation of the two melamine moieties of a calix[4]arene dimelamine. The C^a and C^b carbons are used as probes to analyze the symmetry of the assemblies by ^{13}C NMR spectroscopy.

Recently, we have shown that assemblies of one handedness are formed when chiral centers are present in the building blocks.[15] The C_{3h} and C_s isomers, in which the two melamines (on each calix[4]arene) are in an eclipsed orientation (Figure 2), have a plane of symmetry and are therefore achiral. The C_{3h} and C_s isomers differ in the sense that the C_s isomer lacks a C_3-axis due to the 180° rotation of one of the calix[4]arenes.

Whitesides et al. have previously discussed the value of ^1H NMR spectroscopy as a tool for the analysis of the symmetry of hydrogen-bonded assemblies.[16] Upon the formation of assemblies, the NH protons of the barbiturate or isocyanurate component get involved in hydrogen bonding and undergo a large downfield shift from 8.4 to 13−16 ppm, an area free of other resonances. The number of resonances reflects the symmetry of the assembly. For assemblies such as $\mathbf{1}_3\cdot(DEB)_6$, the C_s isomer can easily be distinguished from the other two isomers. On the basis of symmetry, a total of six proton signals in the 13−16 ppm region of the ^1H NMR spectrum is expected, since all NH_{barb} protons within one rosette layer reside in a different magnetic environment, due to the absence of the C_3-axis. For the D_3 and C_{3h} isomers two signals are expected, as the three different substituents on the melamines render the two NH_{barb} protons of each barbiturate chemically inequivalent in the assembly, thereby giving two anisochronic signals for these protons. Since the two rosette layers are related either by a C_2-axis (D_3 isomer) or a σ_h-plane (C_{3h} isomer), the protons in one rosette layer are either homotopic or enantiotopic, respectively, compared to the protons in the second rosette layer and therefore give identical resonances.[17] The D_3 and C_{3h} isomers can be distinguished using ^{13}C NMR spectroscopy. These isomers differ in the number of signals for the C^a and C^b carbon atoms of the unsubstituted aromatic rings of the calix[4]arene (Figure 2). The C_2-axes in the D_3 isomer cause the C^a and C^b carbons to be homotopic (isochronous), resulting in a single resonance. The C^a and C^b carbons in the C_{3h} isomer, which lacks C_2-axes, are heterotopic (anisochronous) and therefore give different signals. Similarly, the protons H^a and H^b are homotopic in the D_3 isomer and enantiotopic in the C_{3h} isomer, but these protons are occasionally substituted by other groups, thus preventing a general characterization by ^1H NMR spectroscopy.

Structural Variations in the Building Blocks. Structural variations within the components can readily be introduced at three different positions, i.e., positions X, R^1/R^2, and R^3 (Chart 1). We have investigated the formation of assemblies with barbituric acid (BA) and a series of derivatives (5,5-dimethyl- (DMB), 5,5-diethyl- (DEB), and 5-ethyl-5-phenyl- (EPB)) with substituents that differ mainly in size, and one bisbarbiturate (BisBAR) in which the two barbituric acid moieties are connected via a C_3-spacer. Furthermore, the formation of assemblies from a similar series of isocyanuric acid derivatives with butyl (BuCYA), neohexyl (HexCYA), 1,1,1-triphenylpropyl (TripCYA), and *p-tert*-butylphenyl (PheCYA) substituents was investigated.

The influence of the substituents at position R^1 on assembly formation was investigated using calix[4]arene dimelamines **1**, **3**, and **4**, having butyl, benzyl, or (*R*)-1-phenylethyl substituents, respectively. Furthermore, the formation of assemblies from calix[4]arene dimelamine **5**, with one (*R*)-1-phenylethyl and one (*S*)-1-phenylethyl moiety, was investigated. Finally, we examined the effect of the introduction of NO_2 substituents at position R^3 of dimelamine **2** on assembly formation.

Dimelamine **4** was prepared using a procedure similar to that described for dimelamines **1**,[13b] **2**,[13b] and **3**.[13a] For the synthesis of dimelamine **5**, one of the amino groups of **7**[18] was BOC-protected upon reaction with 1 equiv of BOCON to give **8** in 67% yield. Subsequent reaction of **8** with cyanuric chloride (1 equiv, 0 °C) followed by successive reaction with gaseous NH_3 (0 °C) and (*R*)-1-phenylethylamine (6 equiv, reflux) in THF afforded compound **9** in 64% yield. Removal of the BOC group in **9** with TFA gave **10** (93%), which was successively treated with cyanuric chloride (1.1 equiv, 0 °C), gaseous NH_3 (0 °C), and finally (*S*)-1-phenylethylamine (10 equiv, reflux) in THF to give **5** as the final product in an overall yield of 18% (Scheme 1).

Cyanurates BuCYA and PheCYA were synthesized in one step from the corresponding amines via reaction with *N*-chlorocarbonylisocyanate in 15% and 25% yield, respectively, following a literature procedure.[19] The remaining compounds were either commercially available or have been reported previously.[20]

Influence of the Barbituric Acid Substituent X on the Isomeric Distribution. Our initial investigations of the structural isomerism in hydrogen-bonded assemblies were prompted by the observation that all DEB-containing assemblies that we studied form only the D_3 isomer (Table 1 summarizes the isomeric distribution of all assemblies discussed in this paper). As typical examples, the ^1H NMR spectrum and part of the ^{13}C NMR spectrum of assembly $\mathbf{2}_3\cdot(DEB)_6$ are depicted in Figure 3. That assembly $\mathbf{2}_3\cdot(DEB)_6$ exclusively forms the D_3 isomer is confirmed by the presence of only two NH_{barb} resonances at 14.01 and 13.72 ppm in the ^1H NMR spectrum and a single resonance for the C^a and C^b carbons at 141.08 ppm in the ^{13}C NMR spectrum. This is in full agreement with previously reported X-ray crystal diffraction studies and 2D NOESY experiments of assembly $\mathbf{2}_3\cdot(DEB)_6$.[13b] Assemblies $\mathbf{1}_3\cdot(DEB)_6$ and $\mathbf{3}_3\cdot(DEB)_6$ give very similar spectra, which indicates that in these cases the D_3 isomer is also formed exclusively.

(15) Prins, L. J.; Huskens, J.; De Jong, F.; Timmerman, P.; Reinhoudt, D. N. *Nature* **1999**, *398*, 498−502.

(16) Simanek, E. E.; Wazeer, M. I. M.; Mathias, J. P.; Whitesides, G. M. *J. Org. Chem.* **1994**, *59*, 4904−4909.

(17) This is only the case when the substituents on each melamine are identical.

(18) Timmerman, P.; Boerrigter, H.; Verboom, W.; Reinhoudt, D. N. *Recl. Trav. Chim. Pays-Bas* **1995**, *114*, 103−111.

(19) Kimizuka, N.; Kawasaki, T.; Hirata, K.; Kunitake, T. *J. Am. Chem. Soc.* **1998**, *120*, 4094−4104.

(20) For the synthesis of BisBAR, see: Lipkowski, P.; Bielejewska, A.; Kooijman, H.; Spek, A. L.; Timmerman, P.; Reinhoudt, D. N. *Chem. Commun.* **1999**, 1311−1312. For the synthesis of calix[4]arene dimelamine **6**, see ref 22. For the syntheses of HexCYA and TripCYA, see: Mathias, J. P.; Seto, C. T.; Simanek, E. E.; Whitesides, G. M. *J. Am. Chem. Soc.* **1994**, *116*, 1725−1736.

Chart 1

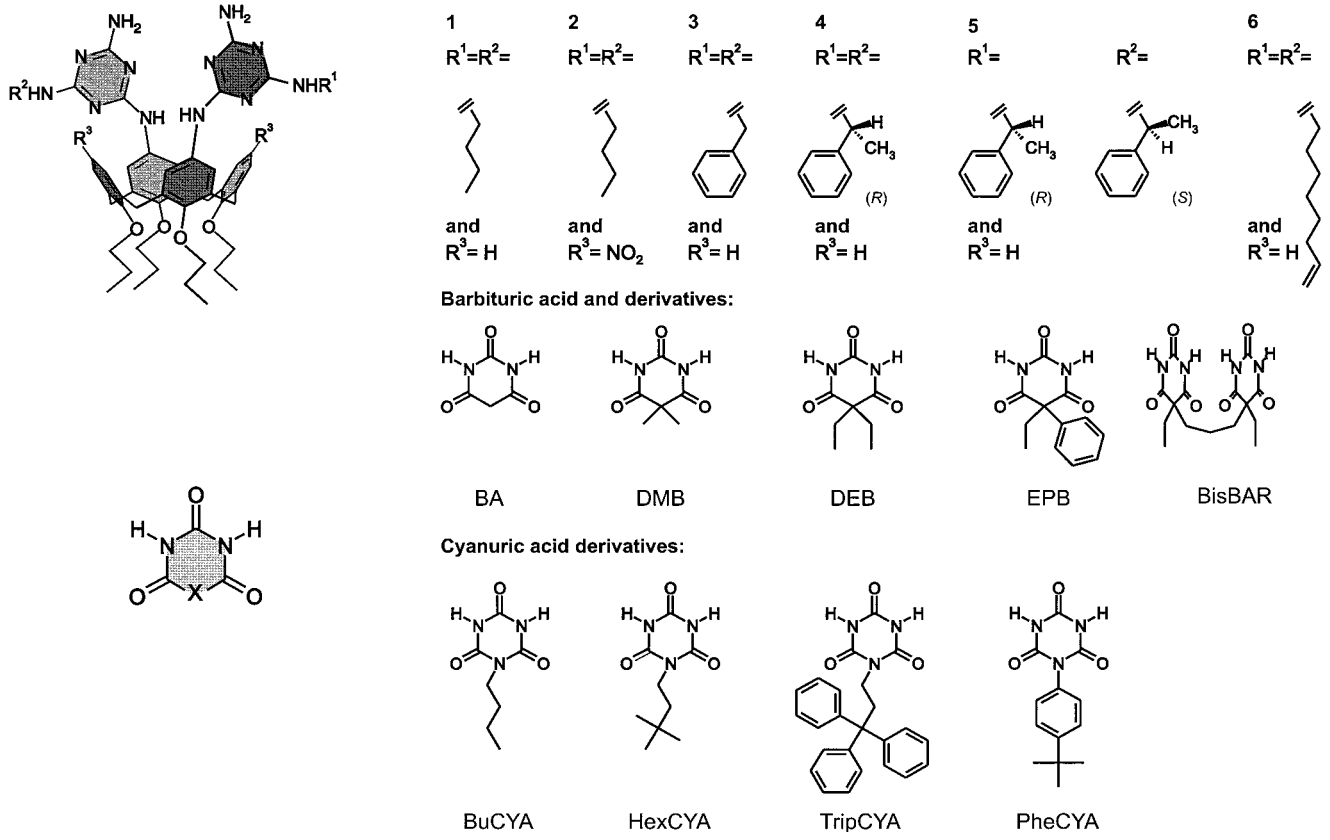

Scheme 1. Synthesis of Calix[4]arene Dimelamine **5**

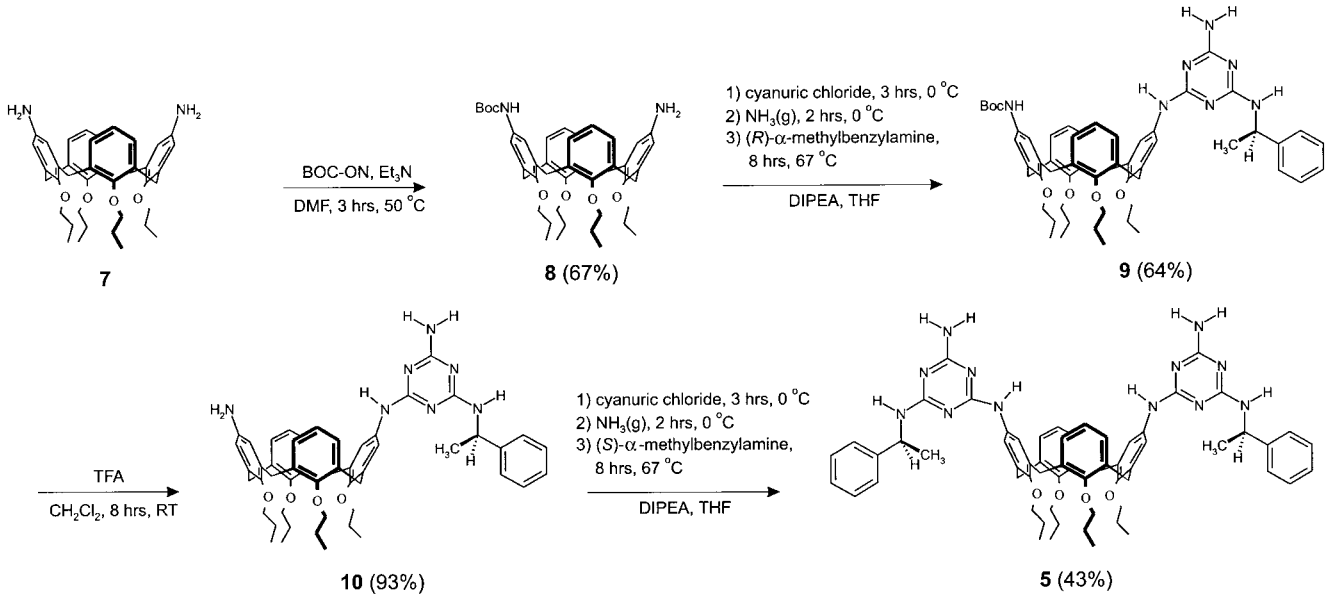

Subsequently, the assembly behavior of a series of closely related barbituric acid derivatives, e.g. DMB, BA, and EPB, was studied. Substitution of both ethyl for methyl groups at position X has no effect on the assembly process. Assembly $\mathbf{2}_3$·$(DMB)_6$ shows two signals in the 13−16 ppm region of the ^{1}H NMR spectrum and one resonance for the C^a and C^b carbons at 141.24 ppm in the ^{13}C NMR spectrum, proving the exclusive formation of the D_3 isomer. For assemblies $\mathbf{1}_3$·$(DMB)_6$ and $\mathbf{3}_3$·$(DMB)_6$ similar results were obtained.

Substitution of DEB by BA gives rise to broad ^{1}H NMR spectra for the assemblies $\mathbf{1}_3$·$(BA)_6$ and $\mathbf{3}_3$·$(BA)_6$, indicating the formation of undefined assemblies. This must be due to a lack of steric bulk at position X, which is essential for the stability of double rosette assemblies. In contrast to this, the ^{1}H NMR spectrum of assembly $\mathbf{2}_3$·$(BA)_6$ is sharp and very similar to assemblies comprising DMB or DEB. The ^{13}C NMR spectrum shows a single resonance for the C^a and C^b carbons, which confirms the presence of the D_3 isomer. The reasons for the very different assembly behavior of dimelamine **2** compared to that of dimelamines **1** and **3** are not entirely clear, but they

Table 1. Summary of the Isomeric Distribution of All Assemblies[a]

calix[4]arene dimelamine	barbiturates					cyanurates			
	DEB	DMB	BA	EPB	BisBAR	BuCYA	PheCYA	HexCYA	TripCYA
1	100/0/0	100/0/0	*b*	100/0/0[c]	*b*	100/0/0	90/5/5	50/20/30	0/90/10
2	100/0/0	100/0/0	100/0/0	100/0/0	0/100/0	100/0/0	*b*	75/15/10	0/10/90
3	100/0/0	100/0/0	*b*	100/0/0[c]	*b*	80/5/15	80/10/10	35/50/15	0/100/0
4	100/0/0	100/0/0	–	100/0/0	–	100/0/0	100/0/0	100/0/0	100/0/0
5	*b*	*d*	–	*b*	–	*d*	0/20/80	0/40/60	*d*
6	100/0/0	–	–	–	–	–	–	–	0/65/35

[a] The relative amounts of the $D_3/C_{3h}/C_s$ isomers are calculated on the basis of the integrals of the signals in the 13−15 ppm region of the ^{1}H NMR spectra. All spectra were recorded at 1 mM concentration in $CDCl_3$. [b] Broad signals were observed, indicating nondefined aggregation. [c] Due to the unsymmetrical orientation of EPB, the two signals for the D_3 isomer are accompanied by relatively broad signals. [d] Sharp signals were observed, indicating well-defined assemblies, but the number of observed signals was higher than theoretically possible.

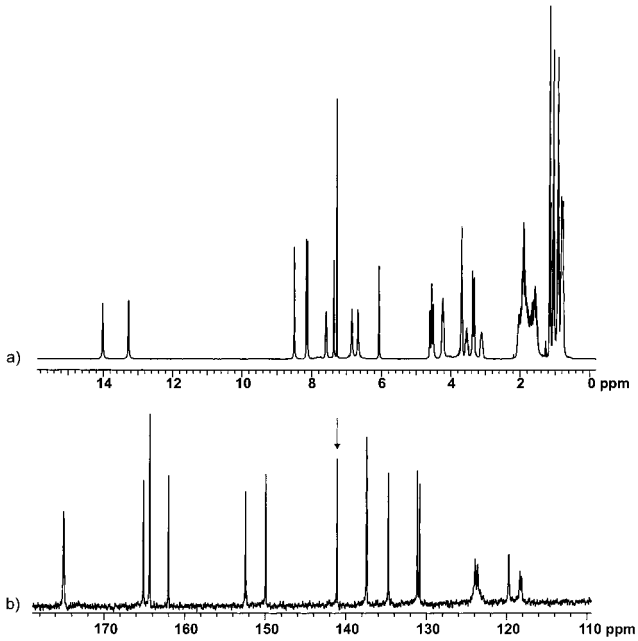

Figure 3. (a) ^{1}H NMR spectrum and (b) part of the ^{13}C NMR spectrum of assembly $\mathbf{2}_3$·$(DEB)_6$. The arrow in the ^{13}C NMR spectrum indicates the signal for the C^a and C^b carbons.

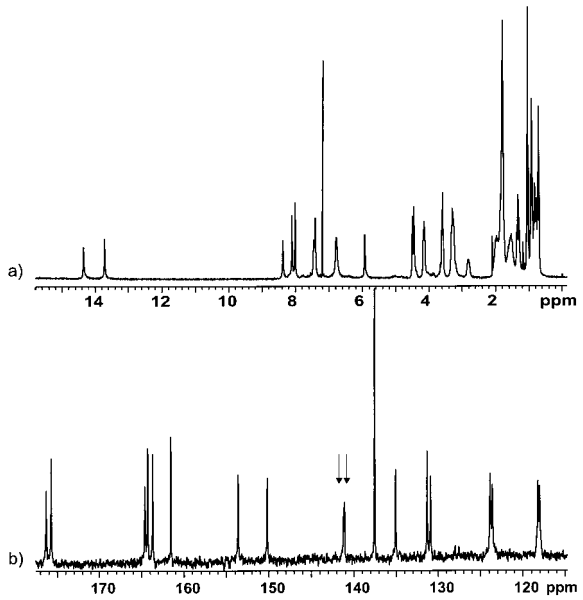

Figure 4. (a) ^{1}H NMR spectrum and (b) part of the ^{13}C NMR spectrum of assembly $\mathbf{2}_3$·$(BisBAR)_3$. The arrows in the ^{13}C NMR spectrum indicate the two signals for the C^a and C^b carbons.

most likely involve a combination of steric and electronic factors, due to the presence of the NO_2 substituents at position R^3.

Assembly $\mathbf{1}_3$·$(EPB)_6$ exhibits two main signals at 13.70 and 14.38 ppm (80% of the intensity) in the 13−16 ppm region of the ^{1}H NMR spectrum together with several small broad signals (20% of intensity). The D_3-symmetrical orientation of the EPBs in which the phenyl groups are pointing away from the assembly is sterically most likely. We assume that the other 20% of the signals is attributed to staggered assemblies in which one or several of the EPBs is oriented upside down, thus destroying the D_3 symmetry. Assembly $\mathbf{3}_3$·$(EPB)_6$ also exhibits two main signals in the 13−16 ppm region (13.59 and 14.15 ppm), but these account for only 60% of the intensity. The remaining 40% is present as relatively broad signals, and the signals are attributed to assemblies with one or several unsymmetrically oriented EPBs. As for the assemblies with BA, dimelamine **2** exhibits a different assembly behavior with EPB compared to dimelamines **1** and **3**. Assembly $\mathbf{2}_3$·$(EPB)_6$ exhibits only two signals (13.59 and 14.21 ppm) in the 13−16 ppm region. No other signals are observed, showing the identical orientation of all EPBs in assembly $\mathbf{2}_3$·$(EPB)_6$.

To obtain information about the intrinsic stability of the C_{3h} and C_s isomers, the assembly behavior of compound BisBAR was studied. The C_3-spacer severely limits the relative freedom of the two barbituric acid moieties and consequently allows the formation of only the eclipsed isomers. The ^{1}H NMR spectrum of assembly $\mathbf{2}_3$·$(BisBAR)_3$ exhibits sharp signals (Figure 4a), with two signals at 13.71 and 14.35 ppm. Together with the two observed signals for the C^a and C^b carbons at 141.21 and 141.10 ppm in the ^{13}C NMR spectrum (Figure 4b), this proves that the assembly is present as the C_{3h} isomer. The ^{1}H NMR spectra of a 1:1 mixture of BisBAR with either dimelamine **1** or **3** show broad resonances, indicating nonspecific hydrogen bonding.

The above results suggest that 5,5-disubstituted barbituric acid derivatives preferentially form the D_3 isomer (DEB, DMB, EPB). Only when formation of the D_3 isomer is sterically impossible, e.g. with BisBAR, is formation of the C_{3h} isomer observed. These results can be rationalized by comparing the position of the barbituric acid substituents in the D_3 isomer and in the C_{3h} and C_s isomers. In the C_{3h} and C_s isomers the two barbituric acid moieties in the upper and lower rosette layer are perfectly aligned, causing steric hindrance between the 5-alkyl substituents of both barbiturate fragments. In the D_3 isomer this steric hindrance is relieved as a result of the staggered orientation of the barbiturate components leaving ample space for the 5-alkyl substituents.

Influence of the Isocyanuric Acid Substituents on the Isomeric Distribution. Isocyanurates have a DAD·DAD hydrogen bonding pattern similar to that of barbiturates, but both the number and the orientation of their substituents is different because they are attached to an sp^2-hybridized nitrogen atom

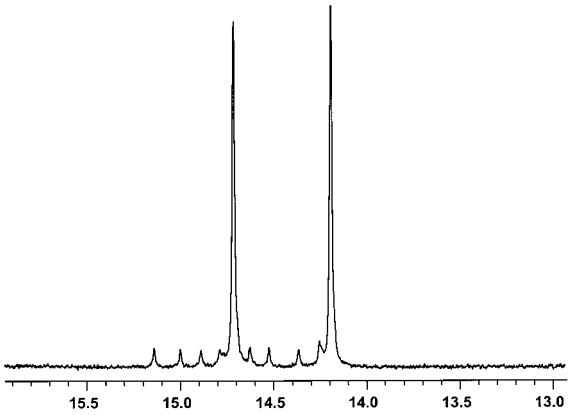

Figure 5. Part of the ^{1}H NMR spectrum of assembly $\mathbf{3}_3$·(BuCYA)$_6$.

instead of an sp^3-hybridized carbon as in the barbiturates. In general, the stability of isocyanurate assemblies is higher since the NH groups are stronger H-bond donors.[21] The increase in hydrogen bonding strength is reflected in the ^{1}H NMR spectra by a stronger downfield shift for the NH$_{cya}$ protons (typically to 14−16 ppm) compared to the NH$_{barb}$ protons (typically to 13−14 ppm) upon assembly.

The isomeric distribution was studied for assemblies comprising isocyanurates BuCYA, PheCYA, HexCYA, and TripCYA. These isocyanurates differ only in the nitrogen substituents, which gradually increase in size.

The ^{1}H NMR spectra of assemblies $\mathbf{1}_3$·(BuCYA)$_6$ and $\mathbf{2}_3$·(BuCYA)$_6$ both show two signals in the 13−16 ppm region. Furthermore, the presence of one single resonance for the C^a and C^b carbons in the ^{13}C NMR spectra of both assemblies (120.55 and 141.10 ppm, respectively) leads to the conclusion that in both cases exclusively the D_3 isomer is formed. Replacing the melamine butyl substituent with a benzyl group, as in assembly $\mathbf{3}_3$·(BuCYA)$_6$, causes a small but significant change. The ^{1}H NMR spectrum exhibits two main signals at 14.72 and 14.19 ppm (80% of the intensity) attributed to the D_3 isomer (Figure 5), accompanied by a total of eight (two + six) sharp signals (20% of the intensity) arising from the corresponding C_{3h} and C_s isomers, respectively. Assembly $\mathbf{3}_3$·(BuCYA)$_6$ is the first example of a double rosette in which all three isomers are observed. Remarkably, the larger size of the benzyl substituent seems to favor the formation of eclipsed isomers.

Assembly $\mathbf{1}_3$·(PheCYA)$_6$ forms almost quantitatively the D_3 isomer according to the ^{1}H and ^{13}C NMR spectra. Assembly $\mathbf{3}_3$·(PheCYA)$_6$ is also formed mainly as the D_3 isomer (80%), but again the eclipsed isomers are observed (20%). Mixing of dimelamine **2** and PheCYA in a 1:2 ratio leads to unspecific hydrogen bonding. CPK models clearly show that, due to the nitro substituents, the periphery of the assembly is sterically too congested to form a double rosette assembly.

A further increase in the size of the isocyanuric acid substituent leads to increased amounts of the C_{3h} and C_s isomers. Assemblies $\mathbf{1}_3$·(HexCYA)$_6$, $\mathbf{2}_3$·(HexCYA)$_6$, and $\mathbf{3}_3$·(HexCYA)$_6$ all show a total of 10 (two + two + six) signals, indicating that all three isomers are present (Figure 6). The ratio between the D_3, C_{3h}, and C_s isomers is 50:20:30, 75:15:10, and 35:50:15, respectively, in the three assemblies. These values confirm our earlier observations that replacement of a butyl for a benzyl group, as in assembly $\mathbf{3}_3$·(HexCYA)$_6$, causes a preference for the C_{3h} isomer, whereas introduction of a nitro group at the C^a and C^b carbons, as in assembly $\mathbf{2}_3$·(HexCYA)$_6$, stabilizes the D_3 isomer.

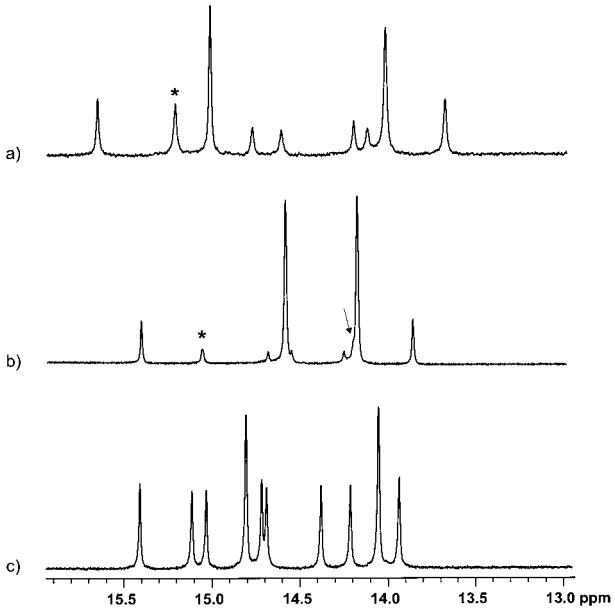

Figure 6. Part of the ^{1}H NMR spectrum of assemblies (a) $\mathbf{1}_3$·(HexCYA)$_6$, (b) $\mathbf{2}_3$·(HexCYA)$_6$, and (c) $\mathbf{3}_3$·(HexCYA)$_6$. The signals marked with an asterisk correspond to two protons indicated by the integration. One of the signals in the spectrum of $\mathbf{2}_3$·(HexCYA)$_6$ is visible as a shoulder of the signal at 14.17 ppm and is indicated by an arrow.

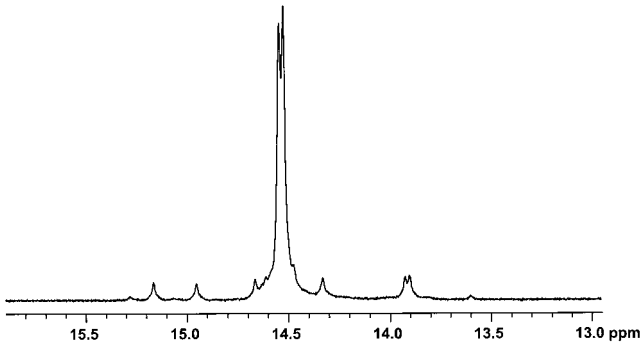

Figure 7. Part of the ^{1}H NMR spectrum of assembly $\mathbf{1}_3$·(TripCYA)$_6$.

The increase in stability of the eclipsed isomers upon increasing the size of the isocyanuric acid substituent becomes even more pronounced for assemblies containing TripCYA, which form mainly as the C_{3h} isomer. The ^{1}H NMR spectra of $\mathbf{1}_3$·(TripCYA)$_6$, $\mathbf{3}_3$·(TripCYA)$_6$, and $\mathbf{6}_3$·(TripCYA)$_6$ all exhibit two main signals at 14.55/14.53, 14.43/14.34, and 14.53/14.44 ppm, respectively. The two signals observed for assemblies $\mathbf{1}_3$·(TripCYA)$_6$ and $\mathbf{6}_3$·(TripCYA)$_6$ are accompanied by six additional signals (10% and 35% of the intensity, respectively) attributed to the C_s isomer (Figure 7). This once more shows how sensitive the assembly process is to changes in the building blocks, since even a seemingly small and negligible change such as the elongation of the alkyl side chains already has a significant effect on the isomeric distribution.

Conclusive evidence for the fact that TripCYA exclusively forms the C_{3h} and C_s isomers was obtained from a covalent capture experiment with assembly $\mathbf{6}_3$·(TripCYA)$_6$ via a ring-closing metathesis (RCM) reaction using the Grubbs catalyst.[22] Recently, we have demonstrated that assembly $\mathbf{6}_3$·(DEB)$_6$, which

(21) Mascal, M.; Fallon, P. S.; Batsanov, A. S.; Heywood, B. R.; Champ, S.; Colclough, M. *J. Chem. Soc., Chem. Commun.* **1995**, 805−806. Shieh, H. S.; Voet, D. *Acta Crystallogr., Sect. B* **1976**, *32*, 3254−3260

(22) Grubbs, R. H.; Chang, S. *Tetrahedron* **1998**, *54*, 4413

Scheme 2. Products of the Covalent Capture of Assembly $\mathbf{6}_3$·(DEB)$_6$ (Trimer **11**[23]) and Assembly $\mathbf{6}_3$·(TripCYA)$_6$ (Monomer **12**) by a RCM Reaction

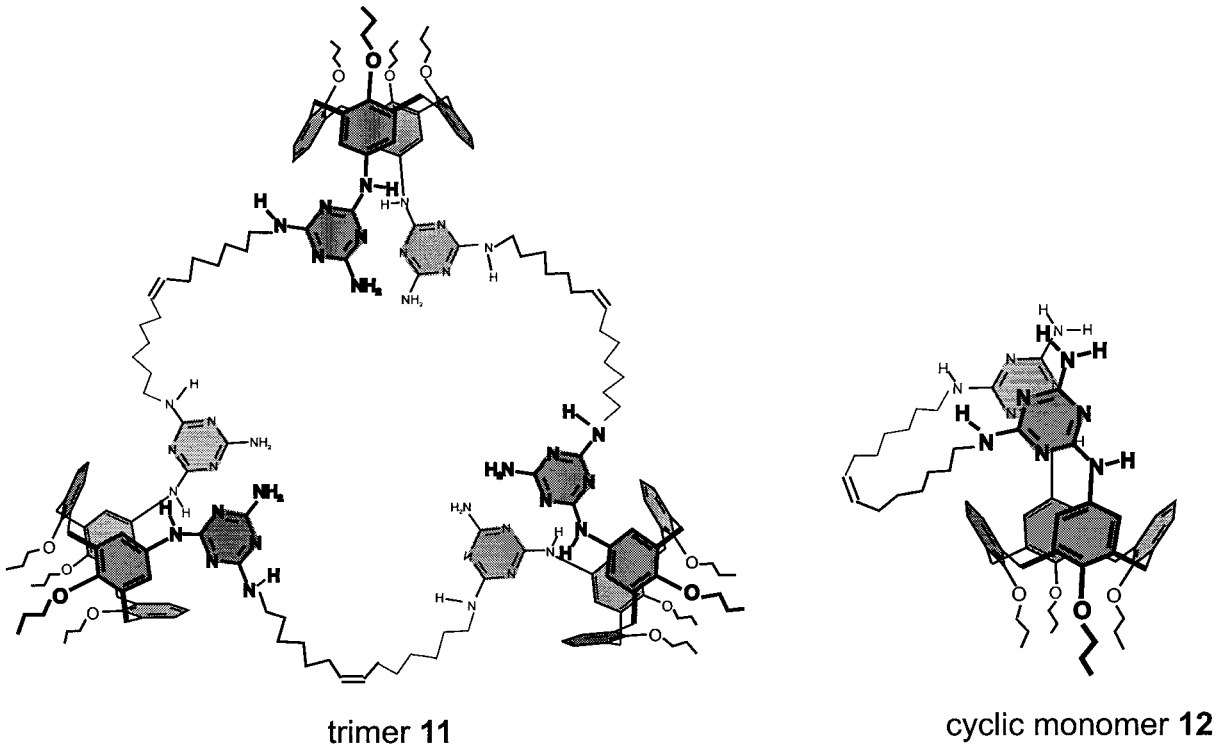

is exclusively present as the D_3 isomer, forms the cyclic trimer **11** in 96% yield, as proven by the signal at $m/z = 3100$ (calcd for $C_{180}H_{240}N_{36}O_{12} = 3100$) in the MALDI-TOF spectrum (Scheme 2).[23] The reason for this is that the alkene moieties within one dimelamine fragment in assembly $\mathbf{6}_3$·(DEB)$_6$ are too remote to react, while the alkene moieties of adjacent dimelamines are in close proximity to each other.

In sharp contrast to this, a RCM reaction with assembly $\mathbf{6}_3$·(TripCYA)$_6$ did not show any trace of the cyclic trimer **11**. Instead, the two alkene moieties of dimelamines react intramolecularly to give cyclic monomer **12** as the only product, proven by the signal at $m/z = 1034.1$ (calcd for $C_{60}H_{80}N_{12}O_4 = 1033.4$) in the FAB-MS spectrum (Scheme 2). This experiment unequivocally proves that the two main signals at 14.53 and 14.44 ppm belong to the C_{3h} instead of the D_3 isomer. Unfortunately, in this case ^{13}C NMR spectroscopy is not a suitable technique to distinguish between the D_3 and the C_{3h} isomers, as it fails to show two signals for the C^a and C^b carbons of assembly $\mathbf{1}_3$·(TripCYA)$_6$, most probably due to a coincidental magnetic equivalence.

Surprisingly, the introduction of a nitro substituent at position R^3 completely interchanges the stabilities of the C_{3h} and C_s isomers. Assembly $\mathbf{2}_3$·(TripCYA)$_6$ almost quantitatively (90%) forms as the C_s isomer, as illustrated by the presence of six signals in the 13−16 ppm region of the ^{1}H NMR spectrum (Figure 8).

The above results clearly show that the outcome of the assembly process is extremely diverse and mostly unpredictable. The isomeric distributions of the assemblies cover the whole spectrum of possible isomeric distributions, ranging from the quantitative formation of the D_3 isomer for assemblies comprising DEB or DMB to the exclusive assembly (90%) of the C_{3h} isomer for assembly $\mathbf{1}_3$·(TripCYA)$_6$, and a nearly quantitative formation of the C_s isomer for assembly $\mathbf{2}_3$·(TripCYA)$_6$. On the other hand, assembly $\mathbf{1}_3$·(HexCYA)$_6$ is formed as a mixture of all three isomers. Steric effects play an important role, as illustrated by the effects of replacing a butyl for a benzyl substituent on the dimelamine or the increase in size of the isocyanurate substituents, but other factors including electronic interactions and solvation effects most likely contribute to the isomeric distribution as well. This has been clearly illustrated by the peculiar assembly behavior of dimelamine **2** and the bulky cyanurate TripCYA.

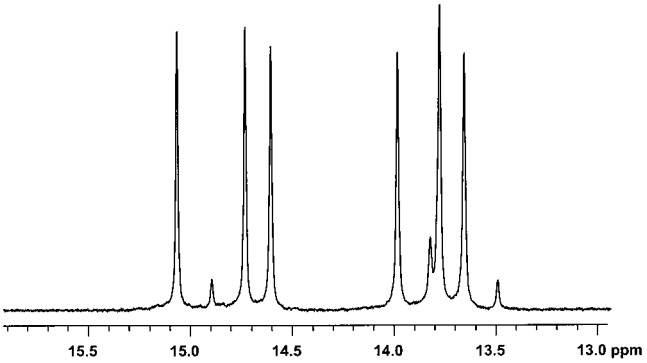

Figure 8. Part of the ^{1}H NMR spectrum of assembly $\mathbf{2}_3$·(TripCYA)$_6$.

Molecular Dynamics Studies. In an attempt to gain visual insight into the assembly process, we performed a series of molecular dynamics (MD) simulations in OPLS $CHCl_3$[24] with assemblies $\mathbf{1}_3$·(DEB)$_6$, $\mathbf{1}_3$·(HexCYA)$_6$, and $\mathbf{1}_3$·(TripCYA)$_6$. These assemblies were observed to form with very different isomeric distributions ($D_3 = 100\%$ for $\mathbf{1}_3$·(DEB)$_6$, $D_3/C_{3h}/C_s =$ 50/20/30% for $\mathbf{1}_3$·(HexCYA)$_6$, and $C_{3h} = 95\%$ for $\mathbf{1}_3$·(TripCYA)$_6$, respectively), although they differ only in the barbiturate/isocyanurate component. For each individual assembly, all three

(23) Cardullo, F.; Crego Calama, M.; Snellink-Ruël, B. H. M.; Weidmann, J.-L.; Bielejewska, A.; Fokkens, R.; Nibbering, N. M. M.; Timmerman, P.; Reinhoudt, D. N. *Chem. Commun.* **2000**, 367−368.

(24) Jorgensen, W. L.; Briggs, J. M.; Contreras, M. L. *J. Phys. Chem.* **1990**, *94*, 1683.

isomers were generated starting from the X-ray crystal structure of assembly $\mathbf{2}_3$·$(DEB)_6$ using Quanta 97.[25] The MD calculations were carried out with CHARMm version 24[26] for a period of 250 ps, after which the structural integrity of the assemblies was examined. The flatness of the rosette motif, rotation of one or more of the melamine/barbiturate fragments out of the rosette motif, and the number of intact hydrogen bonds are regarded as qualitative tools to judge the stability of each of the isomers.[27,28]

After 250 ps, only the D_3 isomer of assembly $\mathbf{1}_3$·$(DEB)_6$ is structurally intact (Figure 9a). In both the C_{3h} and C_s isomers, barbiturate or melamine fragments have rotated away from the assembly, which is clearly visible (Figure 9b,c). This is most likely due to repulsion of the ethyl groups. These results are in agreement with our experimental observation that 5,5-disubstituted barbituric acid derivatives exclusively form the D_3 isomer.

A similar analysis of the three isomers of assembly $\mathbf{1}_3$·$(TripCYA)_6$ after 250 ps shows that only the C_{3h} isomer has 34−36 intact hydrogen bonds and does not show any sign of destruction. In the C_s isomer, steric interactions between the two TripCYAs in the most crowded part of the assembly force an almost 90° deviation of planarity in the rosette motifs. The rosette motifs in the D_3 isomer deviate strongly from planarity as well, but in this case the deviation is due to destructive interactions with solvent molecules. Early in the simulation, two chloroform molecules penetrate between the rosette motifs, breaking the assembly apart (Figure 10). Apparently, the solvation of assembly $\mathbf{1}_3$·$(TripCYA)_6$ in $CHCl_3$ plays an important role in determining the isomeric distribution, with the interior of the D_3 isomer being more accessible to solvent molecules than the eclipsed isomers.

For assembly $\mathbf{1}_3$·$(HexCYA)_6$, all three isomers show nearly flat rosette motifs with 34−36 intact hydrogen bonds after 250 ps. No signs of disruption are observed, while in general the disruptive processes began early in the simulation (0−50ps).

The MD simulations presented here contribute significantly to the visualization of how different parameters affect the isomeric distribution. These studies show that the origin of the destabilization of specific isomers either may be present within the assembly, e.g. steric hindrance, or can arise from direct solvation effects. A quantitative analysis of the MD simulations as well as the use of MD to predict the stability of hydrogen-bonded assemblies in general is currently under investigation.

From the assembly experiments described in this paper, it is evident that small structural variations in the molecular components have an unpredictable effect on the outcome of the assembly process. Although the outcome of the assembly in most cases can be rationalized via MD simulations, it is far more complicated to predict the outcome of the assembly process. This is most clearly illustrated by the opposite effect of increasing steric bulk on the barbiturate and isocyanurate assemblies. Whereas an increase in size of the isocyanurate substituent leads to preferential formation of the eclipsed isomers, the same steric parameter is used to explain induction of the D_3 isomer for barbiturates. In addition to this, electronic interactions and solvation effects are even more difficult to predict.

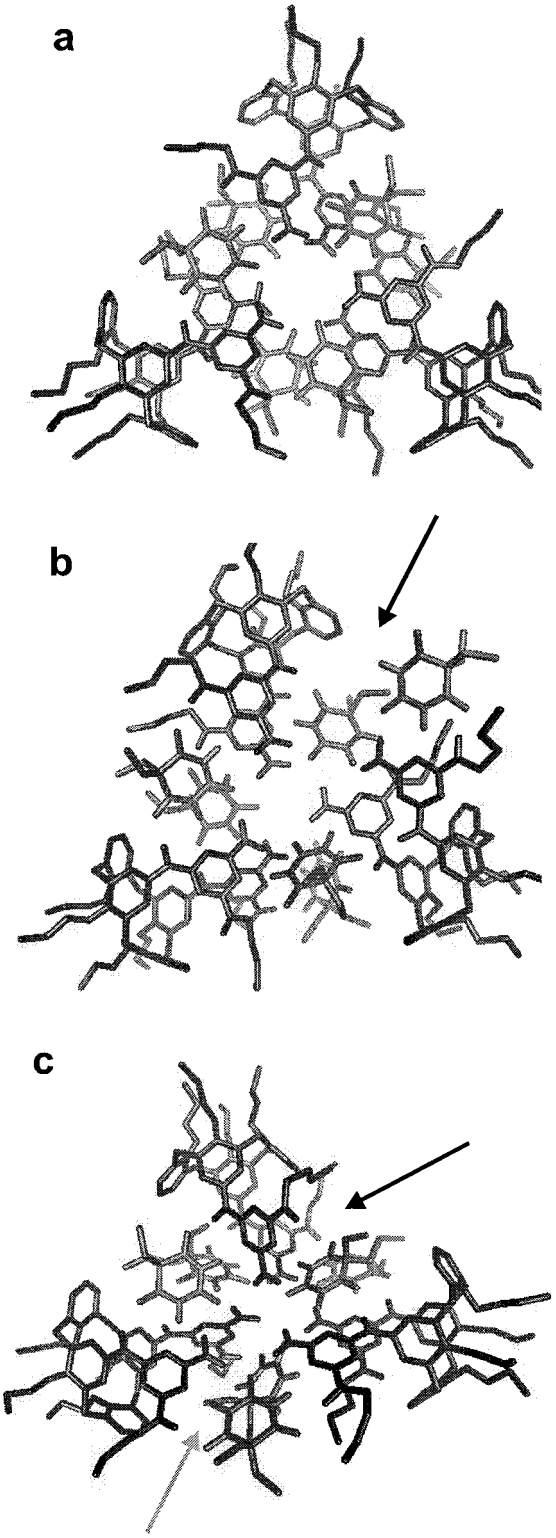

Figure 9. Structures of the (a) D_3, (b) C_{3h}, and (c) C_s isomers of assembly $\mathbf{1}_3$·$(DEB)_6$ after MD runs of 250 ps (top views). Nonpolar hydrogens have been omitted for clarity. The arrows depict places in the assemblies where the structural integrity is lost, due to the expulsion of cyanurate (b) and melamine fragments (c).

Controlling the Isomeric Distribution via Chiral Substituents. The final part of this paper describes a series of experiments demonstrating that the introduction of chiral centers

(25) Quanta 97, Molecular Simulations, Waltham, MA, 1997.

(26) (a) Brooks, B. R.; Bruccoleri, R. E.; Olafsen, B. D.; States, D. J.; Swaminathan, S.; Karplus, M. *J. Comput. Chem.* **1983**, *4*, 187−217. (b) Momany, F. A.; Klimkowski, V. J.; Schäfer, L. *J. Comput. Chem.* **1990**, *11*, 654−662. (c) Momany, F. A.; Rone, R.; Kunz, H.; Frey, R. F.; Newton, S. Q.; Schäfer, L. *J. Mol. Struct.* **1993**, *286*, 1.

(27) Chin, D.; Gordon, D. M.; Whitesides, G. M. *J. Am. Chem. Soc.* **1994**, *116*, 12033−12044.

(28) The number of intact hydrogen bonds for stable structures ranges from 34 to 36, due to the fact that occasionally one or several of the NH_{mel}s in the outer ring of the rosette motif temporarily rotate away.

Figure 10. Structure of the D_3 isomer of assembly $\mathbf{1}_3$·(TripCYA)$_6$ after a MD simulation of 250 ps (top view). Nonpolar hydrogens have been omitted for clarity. Two solvent molecules (van der Waals representation) have penetrated between the rosette layers, causing a disruption of the assembly.

in the building blocks can be used to control the assembly process.[15] As an example we use assembly $\mathbf{3}_3$·(HexCYA)$_6$, which is present as a mixture of the D_3, C_{3h}, and C_s isomers in a 50:20:30 ratio (vide supra, Figure 6a). Substitution of the achiral benzyl substituents in **3** for (*R*)-1-phenylethyl groups, as in **4**, completely changes the outcome of the assembly process. Only the D_3 isomer is formed, as concluded from the presence of the two signals at 13.92 and 14.61 ppm in the ^{1}H NMR spectrum of assembly $\mathbf{4}_3$·(HexCYA)$_6$ (Figure 12a).[29] The reason for this behavior is that the chiral substituents have a strongly preferred orientation with respect to the rosette core (Figure 11a) and are unable to rotate, as revealed by 2D ^{1}H NMR ROESY measurements of assembly $\mathbf{4}_3$·(DEB)$_6$.[14]

Only when the assembly is formed as the D_3 isomer can both chiral substituents adopt the preferred orientation. Similarly, assemblies $\mathbf{4}_3$·(DEB)$_6$ (Figure 12b), $\mathbf{4}_3$·(DMB)$_6$, $\mathbf{4}_3$·(EPB)$_6$, $\mathbf{4}_3$·(BuCYA)$_6$, $\mathbf{4}_3$·(TripCYA)$_6$ and $\mathbf{4}_3$·(PheCYA)$_6$ (Figure 12c) also selectively form the D_3 isomer, even though in some cases the corresponding assembly with achiral dimelamine **3** favors the eclipsed isomers.

Quantitative formation of the C_{3h} and C_s isomers can be achieved with meso dimelamine **5**, in which the two melamines carry substituents of opposite chirality. The ^{1}H NMR spectrum of assembly $\mathbf{5}_3$·(HexCYA)$_6$ exhibits eight signals in the 13−16 ppm region, which proves the exclusive formation of the eclipsed isomers (Figure 12d). No trace of the staggered isomer is observed. This result can similarly be rationalized by examination of the orientation of the chiral substituents. Only for the eclipsed isomers of this assembly can both chiral substituents adopt the energetically most favorable orientation (Figure 11b). Similarly, the selective formation of the C_{3h} and C_s isomers was also observed for assembly $\mathbf{5}_3$·(PheCYA)$_6$ (Figure 12e).

The ^{1}H NMR spectra for mixtures of dimelamine **5** and DEB or EPB show only broad signals (Figure 12f), indicating the formation of undefined assemblies. In these cases the inducing effects of the chiral substituents in **5** oppose the inducing effect of the DEB and EPB components. Dimelamine **5** preferentially

(29) As a result of the presence of the (*R*)-α-methylbenzyl substituents, the C_{3h} isomer no longer contains a σ_h-plane, and therefore four signals are expected for the C_{3h} isomer instead of two.

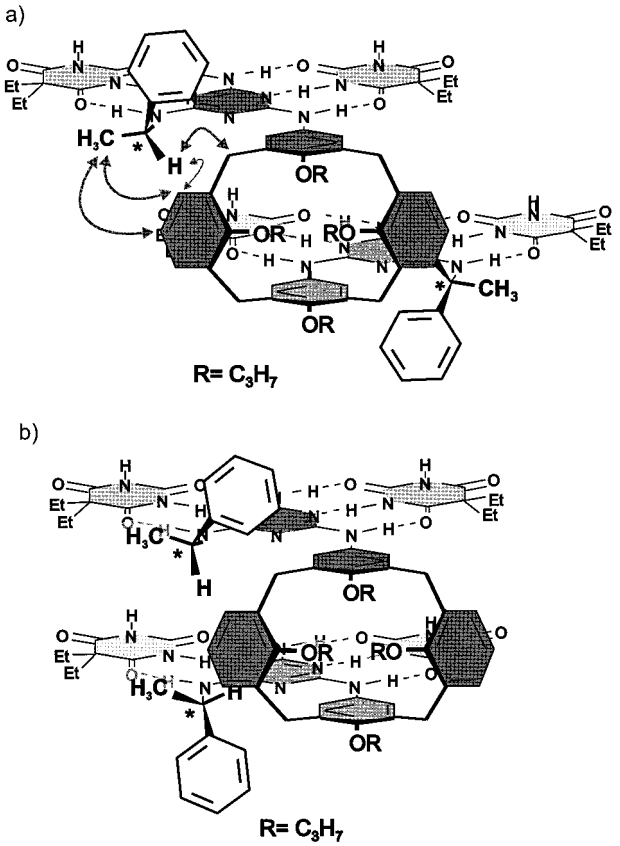

Figure 11. (a) Orientation of the chiral substituents of dimelamine **4** with respect to the rosette core as elucidated from 2D NOESY measurements (NOESY enhancements are indicated by arrows). (b) Corresponding orientation of the chiral substituents of dimelamine **5**.

forms the C_{3h} and C_s isomers, whereas DEB and EPB are observed to form only the D_3 isomer, as a result of steric effects (vide supra). This results in obstruction of the double rosette assembly process, leading to the formation of nondefined assemblies.

The assembly studies with dimelamine **5** and either DMB, BuCYA, or TripCYA show that the inducing effects of the chiral substituents may be occasionally overruled by other factors. All three assemblies exhibit sharp signals in the 13−16 ppm region of the ^{1}H NMR spectrum, indicating the formation of well-defined assemblies. However, the number of observed signals is much larger (15, 14, and 16, respectively) than theoretically possible (12) when all isomers are present. The reason for this assembly behavior remains unclear.

In summary, we can state that chiral substituents can have a strong directing effect on the isomeric distribution of hydrogen-bonded assemblies. The handedness of chiral groups (i.e. (*R*) or (*S*)) can generate an energetic difference between the staggered and eclipsed isomers, resulting in preferential formation of the D_3 isomer in the case of dimelamine **4** and preferential formation of the C_{3h} and C_s isomer in the case of dimelamine **5**.

Conclusions

In this paper we show that the isomeric distribution of noncovalent hydrogen-bonded assemblies can be *controlled* in a predictable manner via the introduction of chiral substituents in the assembly components. We describe the results of a systematic study on the assembly of a series of calix[4]arene dimelamines with barbituric acid and isocyanuric acid derivatives. Analysis of the results using ^{1}H and ^{13}C NMR spectros-

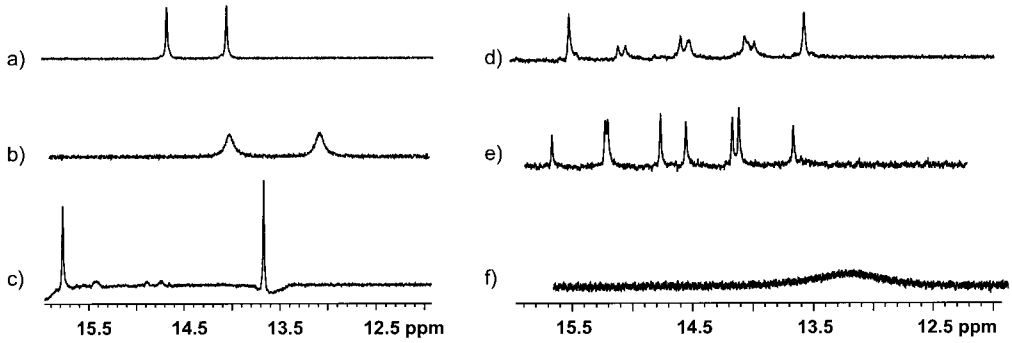

Figure 12. Part of the ^{1}H NMR spectra of assemblies (a) $\mathbf{4}_3$·(HexCYA)$_6$, (b) $\mathbf{4}_3$·(DEB)$_6$, (c) $\mathbf{4}_3$·(PheCYA)$_6$, (d) $\mathbf{5}_3$·(HexCYA)$_6$, (e) $\mathbf{5}_3$·(PheCYA)$_6$, and (f) $\mathbf{5}_3$·(DEB)$_6$.

copy together with MD simulation studies clearly shows that the isomeric distribution between D_3, C_{3h}, and C_s isomers is determined by a combination of different factors, i.e., steric, electronic, and solvation effects. For most assemblies this makes an a priori prediction of the outcome of the assembly process virtually impossible. However, this changes when chiral building blocks are used. It has been shown for the first time that chiral substituents present in the molecular components determine the isomeric distribution of the assembly in a rational manner. We believe that the role of chirality in controlling self-assembly processes will become increasingly important.

Experimental Section

THF was freshly distilled from Na/benzophenone, EtOAc, and hexane (referring to petroleum ether fraction with bp 60−80 °C) from K_2CO_3 and CH_2Cl_2 from $CaCl_2$. All chemicals were of reagent grade and used without further purification. NMR spectra were recorded on a Bruker AC 250 (250 MHz) or a Varian Unity 300 (^{1}H NMR 300 MHz) spectrometer at room temperature. Residual solvent protons were used as internal standard, and chemical shifts are given relative to tetramethylsilane (TMS). FAB-MS spectra were recorded with a Finnigan MAT 90 spectrometer with *m*-nitrobenzyl alcohol (NBA) as a matrix. EI mass spectra were recorded on a Finnigan MAT 90 spectrometer with an ionizing voltage of 70 eV. Elemental analyses were performed using a Carlo Erba EA1106. The presence of solvents in the analytical samples was confirmed by ^{1}H NMR spectroscopy. Flash column chromatography was performed using silica gel (SiO_2, E. Merck, 0.040−0.063 mm, 230−240 mesh).

5,17-*N*,*N*′-Bis[4-amino-6-(*R*)-1-phenylethylamino-1,3,5-triazin-2-yl]diamino-25,26,27,28-tetrapropoxycalix[4]arene (4). This compound was obtained as a white solid (0.58 g, 65%) in a manner similar to the previously reported dimelamine calix[4]arene **1**[13b] starting from 5,17-*N*,*N*′-bis[4-amino-6-chloro-1,3,5-triazin-2-yl]diamino-25,26,27,28-tetrapropoxycalix[4]arene[13b] (0.75 g, 0.85 mmol), (*R*)-α-methylbenzylamine (4.0 mL, 31 mmol), and DIPEA (1.8 mL, 10.3 mmol) in THF (10 mL). ^{1}H NMR (250 MHz, DMSO-d_6): δ 8.5 (br s, 1H, NH), 7.4−7.2 (m, 9H, ArH + NH), 6.2−6.1 (m, 10H, ArH + NH_2), 5.26 (br s, 1H, C*H*CH$_3$), 4.32 and 3.02 (ABq, 8H, ^2J(H,H) = 12.8 Hz, $ArCH_2$-Ar), 3.89 and 3.63 (2t, 8H, ^3J(H,H) = 8.3 Hz, OCH_2), 2.1−1.8 (m, 8H, OCH_2CH_2), 1.42 (d, 3H, ^2J = 6.1 Hz,CHC*H*$_3$), 1.09 and 0.89 (t, 12H, ^3J = 7.4 Hz, $OCH_2CH_2CH_3$). MS (FAB): *m*/*z* 1049.6 ([M + H$^+$], calcd 1049.6). Anal. Calcd for $C_{62}H_{72}O_4N_{12}$·0.2CH_3OH: C, 70.76; H, 6.95; N, 15.92. Found: C, 70.56; H, 6.83; N, 15.85.

5-Amino-17-*N*-(*tert*-butoxycarbamino)-25,26,27,28-tetrapropoxycalix[4]arene (8). A mixture of **7**[18] (0.90 g, 1.45 mmol), BOC-ON (0.36 g, 1.45 mmol), and triethylamine (0.40 mL, 2.87 mmol) in DMF (45 mL) was heated at 50 °C under an argon atmosphere for 3 h and then cooled to room temperature, after which the solvent was removed under reduced pressure. The residue was partitioned between CH_2Cl_2 (100 mL) and aqueous NaOH (1 M, 50 mL), and the aqueous portion was extracted with CH_2Cl_2 (2 × 25 mL). The combined organic solutions were washed with aqueous NaOH (1 M, 2 × 50 mL), water (50 mL), and brine (50 mL) and then dried ($MgSO_4$), and the solvent was removed under reduced pressure to give a yellow oil which was purified by column chromatography (SiO_2; EtOAc/hexane = 1:3). Compound **8** was obtained as a white solid (0.70 g, 67%). ^{1}H NMR (250 MHz, $CDCl_3$): δ 7.4 (br s, 1H, NH), 6.9−6.8 (m, 4H, ArH), 6.7−6.6 (m, 2H, ArH), 6.10 (s, 2H, ArH), 5.68 (s, 2H, ArH), 4.43 and 3.15 (ABq, 4H, ^2J = 16.5 Hz, $ArCH_2Ar$), 4.38 and 3.05 (ABq, 4H, ^2J = 16.1 Hz, $ArCH_2Ar$), 4.0−3.8 (m, 4H, OCH_2), 3.7−3.5 (m, 4H, OCH_2), 2.0−1.7 (m, 8H, OCH_2CH_2), 1.43 (s, 9H, $C(CH_3)_3$), 1.05 and 0.90 (2t, 12H, ^3J = 9.0 Hz). MS (FAB): *m*/*z* 722.9 ([M + H$^+$], calcd 723.4). Anal. Calcd for $C_{45}H_{58}N_2O_6$·0.5H_2O: C, 73.8; H, 8.1; N, 3.8. Found: C, 74.0; H, 8.2; N, 3.9.

5-*N*-[4-Amino-6-(*R*)-1-phenylethylamino-1,3,5-triazin-2-yl]-amino-17-*N*-(*tert*-butoxycarbamino)-25,26,27,28-tetrapropoxycalix[4]-arene (9). To an ice-cold solution of **8** (0.50 g, 0.69 mmol) and DIPEA (0.21 mL, 1.21 mmol) in THF (40 mL) was added cyanuric chloride (0.13 g, 0.70 mmol), and the solution was stirred for 3 h at 0 °C. A stream of ammonia gas was then bubbled through the solution for a period of 2 h, while the temperature was maintained at 0 °C. The solvent was removed under reduced pressure, and the residue was partioned between CH_2Cl_2 (50 mL) and water (50 mL). The organic layer was washed with water (20 mL) and brine (20 mL) and then dried ($MgSO_4$), and the solvent was removed under reduced pressure. Part of the white solid (0.45 g, 0.53 mmol) was redissolved in THF (10 mL), and subsequently DIPEA (0.83 mL, 4.75 mmol) and (*R*)-α-methylbenzylamine (0.70 mL, 5.43 mmol) were added. The mixture was heated at reflux for 2 days, after which the solvent was removed under reduced pressure. The residue was redissolved in CH_2Cl_2 (50 mL), washed with water (50 mL) and brine (50 mL), and subsequently dried (Na_2SO_4). The solvent was removed under reduced pressure, and the resulting yellow solid was purified by column chromatography (silica, EtOAc) to yield **9** as a white solid (0.81 g, 64%). ^{1}H NMR (250 MHz, DMSO-d_6): δ 9.1 (br s, 1H, NH), 8.6 (br s, 1H, NH), 7.4−7.2 (m, 9H, ArH + NH), 6.3−6.2 (m, 8H, ArH + NH_2), 5.27 (t, 1H, ^3J(H,H) = 6.13 Hz, C*H*CH$_3$), 4.33 and 3.06 (ABq, 8H, ^2J(H,H) = 12.8 Hz, $ArCH_2Ar$), 3.90 and 3.63 (2t, 8H, ^3J(H,H) = 7.9 Hz, OCH_2), 2.0−1.7 (m, 8H, OCH_2CH_2), 1.49 (s, 9H, $C(CH_3)_3$), 1.22 (d, 3H, ^2J = 6.13 Hz,CHC*H*$_3$), 1.09 and 0.89 (t, 12H, ^3J = 7.4 Hz, $OCH_2CH_2CH_3$). MS (FAB): *m*/*z* 936.6 ([M + H$^+$], calcd 936.5). Anal. Calcd for $C_{56}H_{69}O_6N_7$: C, 71.77; H, 7.53; N, 10.46. Found: C, 72.15; H, 7.32; N, 10.68.

5-*N*-[4-Amino-6-(*R*)-1-phenylethylamino-1,3,5-triazin-2-yl]amino-17-amino-25,26,27,28-tetrapropoxycalix[4]arene (10). Trifluoroacetic acid (3 mL) was added dropwise to a solution of **9** (0.41 g, 0.44 mmol) in CH_2Cl_2 (30 mL) at 0 °C. The mixture was warmed to room temperature and stirred overnight. Water (20 mL) was then added, followed by portions of solid $NaHCO_3$ until the solution reached pH 7. Subsequently, the mixture was separated, and the organic layer was washed with aqueous NaOH (1 M, 2 × 10 mL) and brine (10 mL) and dried on Na_2SO_4. The solvent was removed under reduced pressure to yield **10** as a white solid (0.34 g, 93%). ^{1}H NMR (250 MHz, DMSO-d_6): δ 8.5 (br s, 1H, NH), 7.4−7.2 (m, 10H, ArH), 6.3−6.2 (m, 10H, ArH + NH + NH_2), 5.26 (br s, 1H, C*H*CH$_3$), 4.54 (br s, 2H, NH_2), 4.29 and 3.00 (ABq, 8H, ^2J(H,H) = 13.2 Hz, $ArCH_2Ar$), 3.9−3.6 (m, 8H, OCH_2), 2.0−1.8 (m, 8H, OCH_2CH_2), 1.43 (d, 3H, ^2J = 6.1 Hz, CHC*H*$_3$), 1.05 and 0.91 (t, 12H, ^3J = 7.4 Hz, $OCH_2CH_2CH_3$). MS

(FAB): *m*/*z* 837.2 ([M + H$^+$], calcd 837.1). Anal. Calcd for $C_{51}H_{61}O_4N_7 \cdot 0.2H_2O$: C, 72.95; H, 7.37; N, 11.68. Found: C, 72.87; H, 7.30; N, 11.36.

5-*N*-[4-Amino-6-(*R*)-1-phenylethylamino-1,3,5-triazin-2-yl]-amino,17-*N*-[4-amino-6-(*S*)-1-phenylethylamino-1,3,5-triazin-2-yl]-amino-25,26,27,28-tetrapropoxycalix[4]arene (5). A procedure similar to that described for the synthesis of **9** was used, starting from **10** (0.34 g, 0.41 mmol), cyanuric chloride (82 mg, 0.44 mmol), and DIPEA (0.2 mL, 1.14 mmol) in THF (25 mL). The intermediate component (0.5 g, 0.5 mmol), (*S*)-α-methylbenzylamine (0.67 mL, 5.2 mmol), and DIPEA (0.92 mL, 5.3 mmol) were refluxed in THF (5 mL) to give **5** as a white solid (0.26 g, 43%) after column chromatography (SiO_2, CH_2Cl_2:MeOH:(25% aqueous NH_3) = 99:9.5:0.5). ^{1}H NMR (250 MHz, DMSO-d_6): δ 8.5 (br s, 1H, NH), 7.4−7.2 (m, 9H, ArH + NH), 6.2−6.1 (m, 10H, ArH + NH_2), 5.26 (br s, 1H, C*H*CH$_3$), 4.32 and 3.02 (ABq, 8H, ^2J(H,H) = 12.8 Hz, $ArCH_2Ar$), 3.89 and 3.63 (2t, 8H, ^3J(H,H) = 8.3 Hz, OCH_2), 2.1−1.8 (m, 8H, OCH_2CH_2), 1.42 (d, 3H, ^2J = 6.1 Hz, CHC*H*$_3$), 1.09 and 0.89 (t, 12H, ^3J = 7.4 Hz, $OCH_2CH_2CH_3$). MS (FAB): *m*/*z* 1049.7 ([M + H$^+$], calcd 1049.6). Anal. Calcd for $C_{62}H_{72}O_4N_{12} \cdot CH_3OH$: C, 69.98; H, 7.08; N, 15.54. Found: C, 69.72; H, 7.20; N, 15.27.

***N*-Butyl-1,3,5-triazine-2,4,6(1*H*,3*H*,5*H*)-trione (BuCYA).** BuCYA was prepared by following a literature procedure to give 5-substituted cyanuric acid derivatives.[19] ^{1}H NMR (300 MHz): δ 11.36 (s, 2H, NH), 3.61 (m, 2H, NCH_2), 1.44 (m, 2H, NCH_2CH_2), 1.26 (m, 2H, $NCH_2CH_2CH_2$), 0.86 (t, 3H, ^3J = 7.3 Hz, CH^3). MS (FAB): *m*/*z* 186.1 ([M + H$^+$], calcd 186.1). Anal. Calcd for $C_7H_{11}O_3N_3 \cdot 0.1CH_3OH$: C, 45.27; H, 6.10; N, 22.31. Found: C, 44.92; H, 6.02; N, 22.31.

***N*-(*p*-*tert*-Butylphenyl)-1,3,5-triazine-2,4,6(1*H*,3*H*,5*H*)-trione (PheCYA).** PheCYA was prepared by following a literature procedure to give 5-substituted cyanuric acid derivatives.[19] ^{1}H NMR (300 MHz, DMSO-d_6) δ 11.51 (s, 2H, NH), 7.45 (d, 2H, ^2J = 8.4 Hz, ArH), 7.22 (d, 2H, ^2J = 8.4 Hz, ArH) 1.30 (s, 9H, $C(CH_3)_3$). MS (EI): *m*/*z* 261.9 ([M + H$^+$], calcd 262.1). Anal. Calcd for $C_{13}H_{15}N_3O_3$: C, 59.8; H, 5.8; N, 15.8. Found: C, 59.7; H, 5.8; N, 15.8.

Assembly Preparation. Typically, 1 mM solutions of assemblies were prepared either by stirring the calix[4]arene dimelamine and barbiturate/cyanurate components overnight in 1.0 mL of $CDCl_3$ or by dissolving both components in THF, evaporating THF, drying under high vacuum, and subsequently resolvating in $CDCl_3$.

RCM Reaction on Assembly 6_3·(TripCYA)$_6$. Ring-closing metathesis (RCM) reactions were performed in toluene-d_8 and were monitored by ^{1}H NMR spectroscopy. Conditions in toluene-d_8: room temperature; 48 h; $[\mathbf{6}]_0$ = 6.0 mM; $[\text{TripCYA}]/[\mathbf{6}]_{t=0}$ = 2.5; $[\text{catalyst}]_{t=0}$ = 0.6 mol %; reactions were quenched by bubbling with oxygen.

Molecular Dynamics Calculations. Initial structures, created by manual modification of the X-ray crystal structure of assembly $\mathbf{2}_3$·(DEB)$_6$,[13b] as well as visualizations were carried out with Quanta 97.[25] The MD calculations were run with CHARMm, version 24.0.[26] Parameters were taken from Quanta 97, and point charges were assigned with the charge template option in Quanta/CHARMm; excess charge was smoothened, rendering overall neutral residues. The structures were placed in a cubic box of approximately 66.0 Å dimensions, initially filled with 2136 OPLS chloroform.[25] Solvent molecules that overlap with the complexes were removed (based on heavy atom interatomic distances of 2.3 Å). Full periodic boundary conditions were imposed. Before the MD simulations were run, the system was minimized by steepest descent, to remove the worst contacts, until the rms on the energy gradient was ≤1.0 kcal·mol^{-1}·Å^{-2} or a maximum of 1000 steps was reached.

During the simulation the nonbonded list was updated every 20 time steps with a cutoff of 12 Å. The van der Waals interactions were treated with a switch function between 10 and 11 Å, whereas the shift function was applied to the electrostatic interactions (cutoff 11 Å). A constant dielectric constant and an ϵ value of 1 were applied. The system was heated to 300 K in 5 ps, followed by 10 ps for equilibration with scaling of the velocities within a temperature window of 10 deg. After equilibration, no scaling of the velocities was applied. The production phase lasted 250 ps, and coordinates were saved regularly for subsequent analysis. The verlet/leapfrog algorithm was used for the numerical integration. The SHAKE algorithm[30] on bonds involving hydrogen was applied, allowing a time step of 1 fs.

Acknowledgment. Prof. R. Glaser is gratefully acknowledged for helpful discussions. Dr. F. Cardullo is acknowledged for providing compound **6** and for assistance with the RCM experiments. Dr. P. Lipkowski is acknowledged for providing compound BisBAR. This research has been financially supported by the Council for Chemical Sciences of The Netherlands Organization for Scientific Research (CW-NWO) (L.J.P) and the Japan Science and Technology Corp. (Chemotransfiguration Project) (K.A.J.).

JA9936262

(30) Berendsen, H. J. C.; Postma, J. P. M.; Dinola, A.; van Gunsteren, W. F.; Haak, J. R. *J. Chem. Phys.* **1984**, *81*, 3684−3690.